American Journal of Renewable and Sustainable Energy
Vol. 4, No. 2, 2018, pp. 24-32
http://www.aiscience.org/journal/ajrse
ISSN: 2381-7437 (Print); ISSN: 2381-7445 (Online)

Thermal Performance of Solar Air Heater Having Absorber Roughened by Chamfered-Square Elements

Man Singh Azad[1], Dipankar Chatterjee[1, *], Apurba Layek[2], Dilip Kumar Biswas[1]

[1]CSIR-Central Mechanical Engineering Research Institute, Durgapur, India
[2]Department of Mechanical Engineering, National Institute of Technology, Durgapur, India

Abstract

In an objective to improve the thermo hydraulic performance of a solar air heater, a novel idea is proposed in this paper following a passive heat transfer enhancement technique. The technique uses the concept of providing artificial roughness on the absorber plate of the heater with diagonally cut cuboids. A numerical study using a computational fluid dynamics (CFD) method is performed to show the enhancement of the thermo hydraulic performance of the heater for the relative roughness pitch of 6 to 8 and cross section of cuboids from 8mm to 12mm with a constant relative roughness height of 0.0889. The Reynolds number is kept in the range of 5000 to 22500 with a constant heat flux of 1000 W/m^2 on the absorber plate. The standard k-ε turbulence model with enhanced wall treatment is used to handle the flow turbulence. The Nusselt number and the average friction factor are determined for different values of the relative roughness pitch and cross sectional areas of the roughness element. In order to determine the enhancement of heat transfer and increment in the friction factor, the Nusselt number and friction factor are compared with those of smooth duct under similar flow conditions. It is observed that the thermal performance of the heater is increased in presence of the chamfered square roughness elements.

Keywords

Solar Air Heater, CFD, Artificial Roughness, Thermal Performance, Overall Enhancement Ratio

Received: April 17, 2018 / Accepted: May 14, 2018 / Published online: June 7, 2018

1. Introduction

As there is a continuous increase in the energy demand, we are encouraged to think new ways to fulfil this demand. Among all the sources of energy, solar energy is freely available to curb this demand. Solar air heating is a solar thermal technology in which the energy from the Sun, (insolation) is captured by an absorbing medium and used to heat air. It is a renewable energy heating technology used to heat or condition air for buildings or process heat applications. It is typically the most cost-effective technology out of all the available solar technologies, and finds the largest usage in space heating and industrial process heating. The efficiency of a solar air heater (SAH) is substantially poor due to low value of heat transfer coefficient between the absorber plate and the working fluid even for the turbulent flow. Several methods have so far been used to increase the rate of heat transfer and the thermal efficiency. Some of these are, use of fins [1-4], electro hydrodynamic method [5], packed bed [6], use of artificial roughness on absorber plate [7-11] etc. Among these, the easiest and the most acceptable method to enhance the thermal performance is the creation of

* Corresponding author
E-mail address: rsdchat@gmail.com (D. Chatterjee)

artificial roughness on the absorber plate of the solar air heater.

It is observed that the thermal resistance to heat transfer is caused due to the formation of the laminar sub-layer on the absorber plate. Artificial roughness elements are used to improve the convective heat transfer by creating turbulence in the flow. However, it would result an increase in the friction losses and hence, greater power requirement by the fan or blower. Various researchers have investigated the thermo-hydraulic performances of solar air heater embedded with different types of artificial roughness elements with an emphasis on the effect of different roughness parameters. These are comprehensively reviewed in Kumar et al. [9] and not repeated here for the purpose of brevity. Another article of Yadav and Thapak [12] is worth mentioning, which provides an excellent review on the available investigations of artificially roughened solar air heater.

Vyas and Shringi [13] performed CFD based analysis on the thermal performance of the solar air heater using baffles as roughness elements and found 2.23 times more heat transfer compared to smooth plates. Vikrant et al. [14] investigated numerically the thermal performance of solar air heater equipped with an artificial roughened surface using circular transverse wire ribs and found considerable heat transfer enhancement. Prasad and Saini [15] used small diameter wire as the roughness element in solar air heater. They investigated the effect of relative roughness height and pitch on the heat transfer and friction factor obtained from empirical correlations. Maximum value of Nusselt number and friction factor were reported as 2.38 and 4.25, respectively for relative roughness pitch of 10. Karwa et al. [16] performed experimental study using v-discrete and v-discontinuous rib and reported that discrete ribs perform better than the discontinuous rib and 60° ribs performed better than 45^{v} ribs. In another article, Karwa and Srivastava [17] reported the mathematical analysis of the thermal performance of a solar air heater with v-down discrete rib roughness. They observed that the thermal efficiency of the roughened duct air heater is higher than that of a smooth duct air heater and the highest advantage was obtained at the lowest flow rate. Later, Gawande et al. [18] performed mathematical modeling and simulation of solar air heater roughened with 20° angled rib for predicting the optimal design and operating parameters.

It is observed that majority of the works available in the literature except a few are experimental. A numerical analysis can be used successfully as an alternative to the expensive experimental investigation and in quick time several different orientations can be studied for their effectiveness in order to enhance the thermal performance of the heater. Accordingly, a novel approach is adopted here to use diagonally chamfered square elements to be inserted artificially on the absorber plate of the heater for making it rough. A numerical study based on the CFD approach is proposed to investigate the effectiveness of the roughness element for improved thermal performance of the heater.

2. Material and Method

Diagonally chamfered square elements of 8 mm to 12 mm arm are used to make artificial roughness on the inner-side of the absorber plate. Different pitch values are used between the ribs. Hydraulic diameter (D) of duct is taken as 45 mm. Solar air heaters normally operate in the range of Reynolds number (Re) 5000 to 22500, so this range has been used to study the effect on heat transfer and friction factor. A uniform heat flux of 1000 W/m^2 is applied on the absorber plate.

The chamfered-cuboid roughness elements are fixed on the inner side of the absorber plate as depicted in figure 1(a). Other three sides of the test section except the absorber plate are considered as smooth surfaces. The solution domain used for the CFD analysis is shown in figure 1(b). The duct used for the CFD analysis is having the height (H) of 25 mm and width (W) of 200 mm. The aspect ratio of the duct is kept 8 in this study. The flow domain consists of 725 mm long entry section, 1000 mm long test section and 375 mm long exit section. The entry and exit lengths of the flow domain are kept sufficiently large to reduce the end effects.

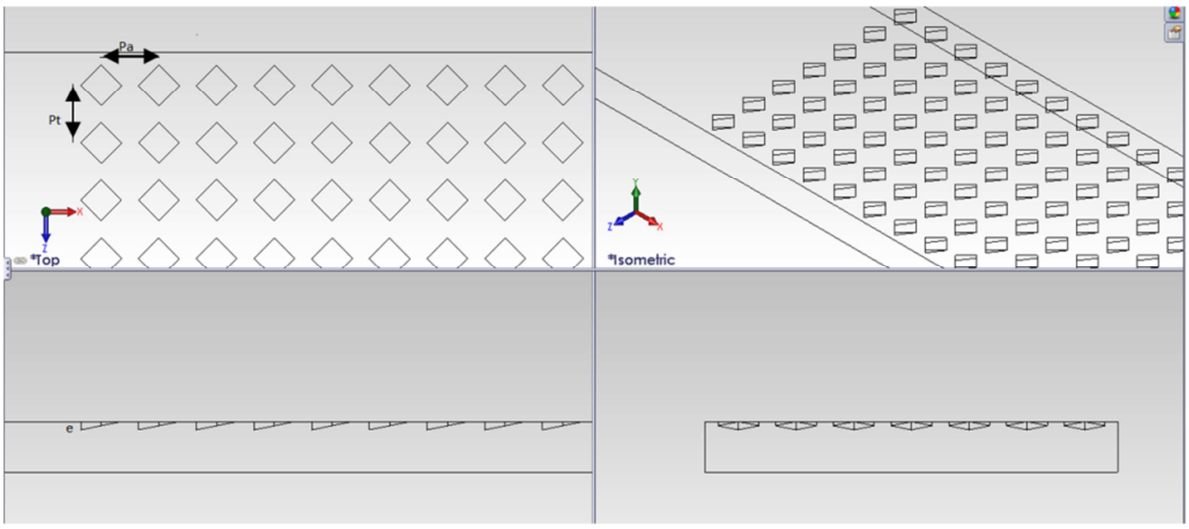

(a)

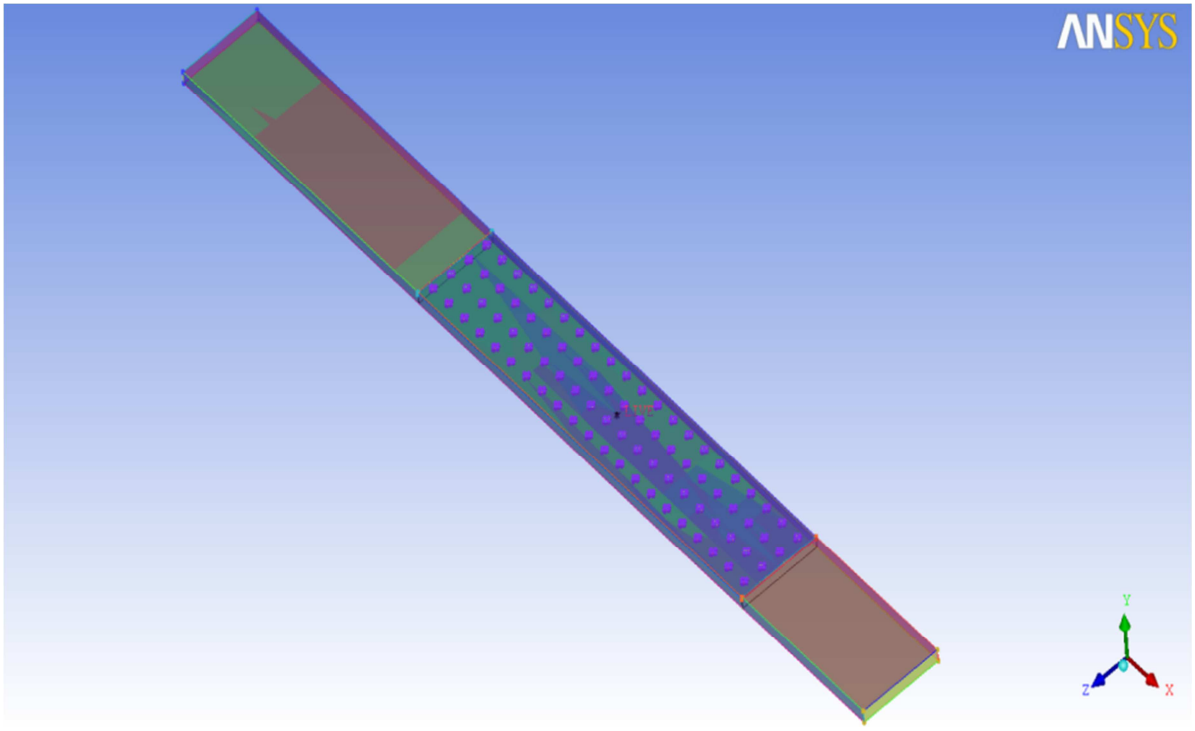

(b)

Figure 1. (a) Geometry and (b) computational domain for the simulation study.

As the roughness geometry is inclined in the transverse direction, secondary flows are bound to happen, thus a 3-D flow domain is selected. In order to examine the flow and heat transfer accurately in the inter-rib regions, finer meshing at these locations are done. In other regions coarser mesh are used. For the present work, meshing is done using ICEM CFD of ANSYS 13.0 [19].

The system of governing equation consists of the continuity, momentum and energy equations. The 3-D forms of the governing equations are shown below:

Continuity equation:

$$\frac{\partial u}{\partial x}+\frac{\partial v}{\partial y}+\frac{\partial w}{\partial z}=0 \tag{1}$$

Momentum equation:

$$u\frac{\partial u}{\partial x}+v\frac{\partial u}{\partial y}+w\frac{\partial u}{\partial z}=-\frac{1}{\rho}\frac{\partial p}{\partial x}+\nu\left(\frac{\partial^2 u}{\partial x^2}+\frac{\partial^2 u}{\partial y^2}+\frac{\partial^2 u}{\partial z^2}\right) \tag{2}$$

$$u\frac{\partial v}{\partial x}+v\frac{\partial v}{\partial y}+w\frac{\partial v}{\partial z}=-\frac{1}{\rho}\frac{\partial p}{\partial y}+\nu\left(\frac{\partial^2 v}{\partial x^2}+\frac{\partial^2 v}{\partial y^2}+\frac{\partial^2 v}{\partial z^2}\right)+g\beta\left(T-T_\infty\right) \tag{3}$$

$$u\frac{\partial w}{\partial x}+v\frac{\partial w}{\partial y}+w\frac{\partial w}{\partial z}=-\frac{1}{\rho}\frac{\partial p}{\partial z}+\nu\left(\frac{\partial^2 w}{\partial x^2}+\frac{\partial^2 w}{\partial y^2}+\frac{\partial^2 w}{\partial z^2}\right) \quad (4)$$

Energy equation:

$$u\frac{\partial T}{\partial x}+v\frac{\partial T}{\partial y}+w\frac{\partial T}{\partial z}=\alpha\left(\frac{\partial^2 T}{\partial x^2}+\frac{\partial^2 T}{\partial y^2}+\frac{\partial^2 T}{\partial z^2}\right) \quad (5)$$

where u, v, w are the fluid velocity components along x, y and z directions of the rectangular Cartesian coordinate, p is the pressure, T is the temperature and T_∞ is the ambient temperature, the thermophysical properties are described through the density (ρ), kinematic viscosity (ν), thermal diffusivity ($\alpha = k/\rho C_p$) with k being the thermal conductivity and C_p the specific heat at constant pressure, β is the volumetric thermal expansion coefficient and g is the acceleration due to gravity.

The thermophysical properties of the working fluid and the absorbed plate are given in Table 1.

Table 1. Thermo-physical properties of working fluid and absorber plate.

Parameter	Fluid (air)	Absorber plate (aluminum)
Specific heat (C_p, J/kg.K)	1004.9	871.00
Thermal conductivity (k, W/m.K)	0.02624	202.40
Density (ρ, kg/m^3)	1.225	2719.00
Viscosity (μ, N/m^2)	1.846x10^5	-
Thermal expansion coefficient (β, K^{-1})	0.0034	-

ANSYS FLUENT Version 13.0 [19] is used for the computational analysis of the solar air heater duct in the present study. A 3-D model is used instead of 2-D model as the secondary flows occur in the duct. The following assumptions are hold: fluid flow is fully developed, steady, and turbulent; the remaining duct walls except the absorber plat are considered adiabatic; and the air (working fluid) is incompressible for the operating range of the solar air heater. These assumptions are made with respect to the experimental investigation done previously on the solar air heater by other investigators.

At the inlet of the solution domain velocity boundary condition is used and outflow boundary condition at the outlet. Turbulence intensity and hydraulic diameter are used to specify the turbulence. Constant heat flux wall boundary condition is applied on the absorber plate. Discretization of the governing equations is done using the second order upwind numerical scheme and the SIMPLE (semi-implicit method for pressure linked equations) algorithm is used for the pressure-velocity coupling.

3. Selection and Validation of Model

To select the appropriate turbulence model for the computational analysis and to validate the model, the predictions of different turbulence models namely the Realizable (RLG) k-ε model and Standard (STD) k-ε model for smooth duct having same cross section are compared with Dittus-Boelter empirical correlation [20] for the Nusselt number and modified Blasius equation for the friction factor.

Dittus-Boelter correlation for smooth duct:

$$Nu = 0.024\,\mathrm{Re}^{0.8}\,\mathrm{Pr}^{0.4} \quad (6)$$

Modified Blasius equation:

$$f_s = 0.085\,\mathrm{Re}^{-0.25} \quad (7)$$

The prediction of Standard (Std) k-ε turbulence model is found to have good agreement with the results of Dittus-Boelter empirical correlation and the modified Blasius equation. Figure 2 shows the variation of the Nusselt number with the Reynolds number for smooth duct predicted by different turbulence models and compared with the Dittus-Boelter correlation results. Similarly, figure 3 shows the variation of the friction factor with Reynolds number for smooth duct predicted by different turbulence models and compared with the modified Blasius correlation results.

The values of the Nusselt number and friction co-efficient with respect to the Reynolds number for the STD k-ε tubulance model are within 5% devition from the corresponding values predicted from the Dittus-Boelter correlation and modified Blasius correlation respectively which is in an acceptable limit. Therefore after this validation STD k-ε tubulant model is selected for the CFD analysis of the solar air heater duct.

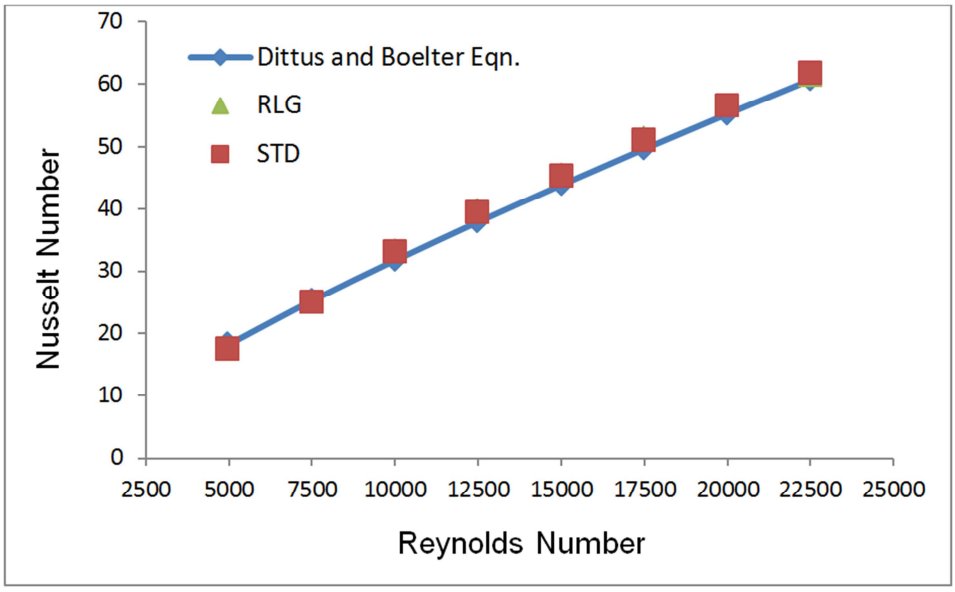

Figure 2. Comparison of Nusselt number predicted by different turbulence models with the Dittus-Boelter relation for smooth duct.

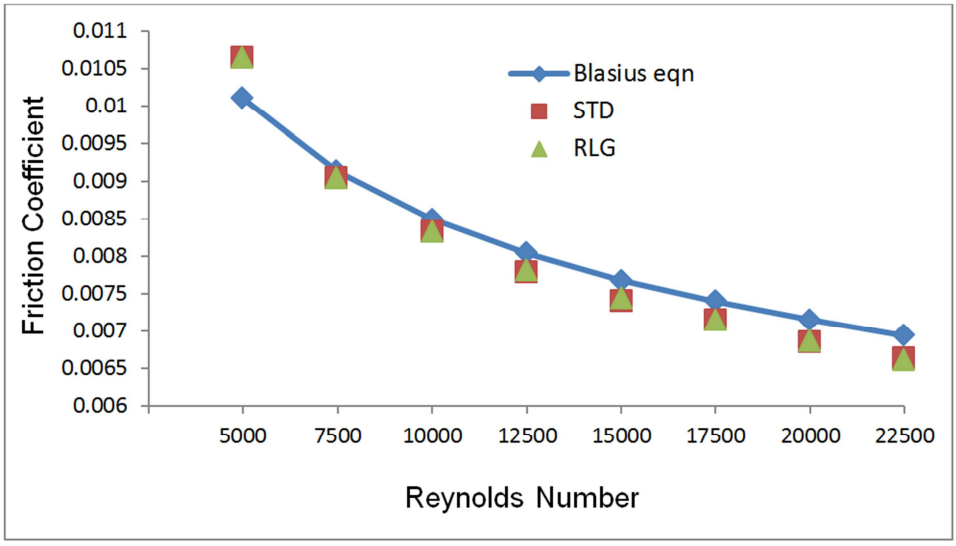

Figure 3. Comparison of friction coefficient predicted by different turbulence models with the modified Blasius relation for smooth duct.

4. Results and Discussion

The results of the roughened plate simulation are presented and compared with the smooth plate. The enhancement of the thermal hydraulic performance of the heater for variable flow rate is discussed below.

4.1. Heat Transfer

The thermal behavior of the SAH is characterized by the Nusselt number against variable Reynolds number. Nusselt number increases with increase in Reynolds number of roughened as well as smooth plate as shown in figures 4 and 5. Figure 4 shows the Nusselt number variation with Reynolds number for different relative roughness pitch (longitudinal pitch, Pa/e = 6, 7 and transverse pitch, Pt/e = 4, 6, 7, 8) and for a fixed cross section of the roughness element (8×4: arm×height). In figure 5, the Nusselt number variation is shown with respect to the Reynolds number for fixed longitudinal and transverse relative roughness pitch (Pa/e = 7, Pt/e = 7). It is also observed from both the figures that the Nusselt number increases with increase in the relative roughness pitch and cross sectional area. The most important observation from the two figures is that the heat transfer increases substantially for the roughened plate in comparison to the smooth plate. Hence, the solar air heater embedded with the artificial roughness element is found to be more effective in a sense that it provides enhanced thermal performance. The highest Nusselt number is found as 84.3 at Pa/e = 7, Pt/e = 7 (with cross section 12×4).

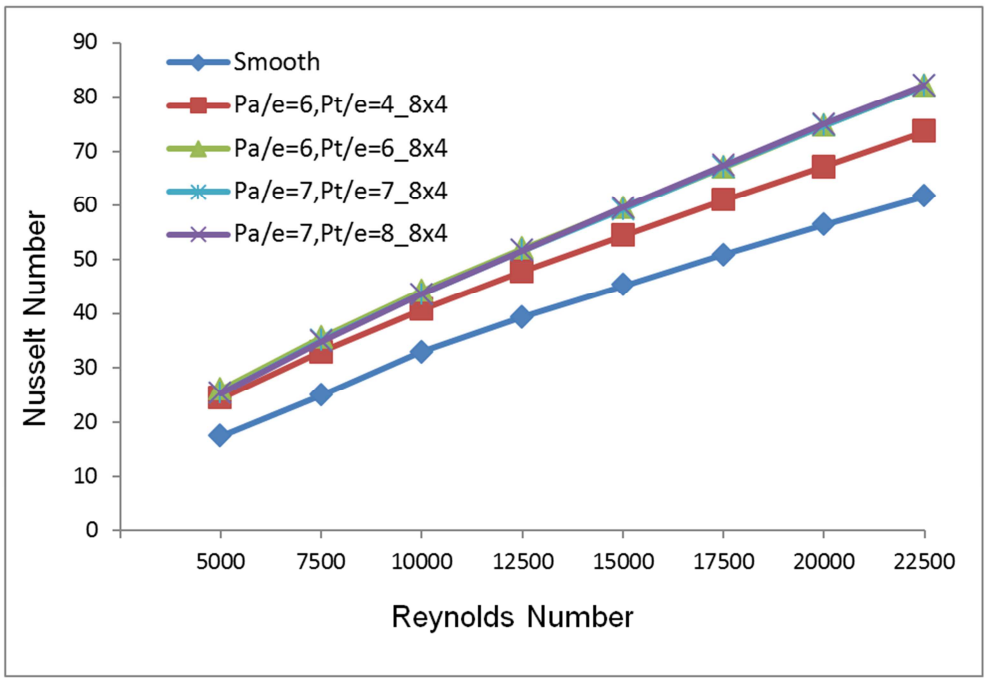

Figure 4. Comparison of Nusselt Number for different relative roughness pitch having fixed element size with smooth duct.

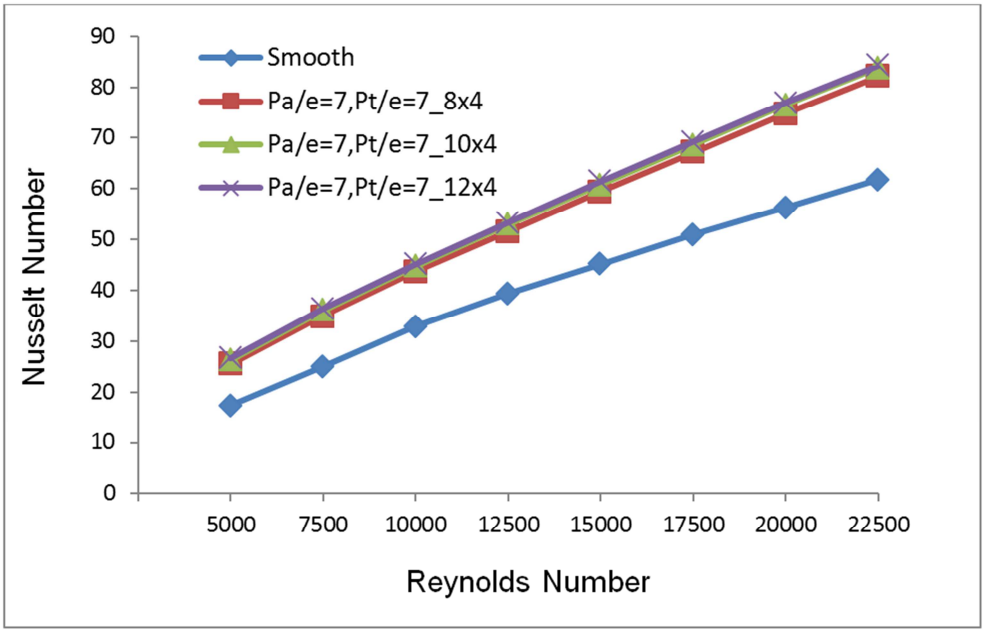

Figure 5. Comparison of Nusselt Number for different element size having fixed relative roughness pitch with smooth Duct.

4.2. Friction Factor

The effect of roughness on flow friction factor in the simulated range of Reynolds number is shown in figures 6 and 7. Figure 6 shows the variation of the friction coefficient with Reynolds number for different relative roughness pitch (longitudinal pitch, Pa/e = 6, 7 and transverse pitch, Pt/e = 4, 6, 7, 8) at fixed cross section of the roughness element (8×4: arm×height). In figure 7, the friction coefficient varies with Reynolds number for different cross section of the roughness element (8×4, 10×4 and 12×4) at fixed longitudinal and transverse relative roughness pitch (Pa/e = 7, Pt/e = 7). The friction factor decreases with increase in Reynolds number due to suppression of laminar sublayer for fully developed turbulent flow in the duct. The maximum average friction factor for the rough plate is found to be 0.0146 at Re = 5000 for Pa/e = 7, Pt/e = 7 (with cross section 12×4) and the minimum average friction factor is obtained as 0.00764 at Re = 22500 for Pa/e = 6 and Pt/e = 4 (with cross section 8×4).

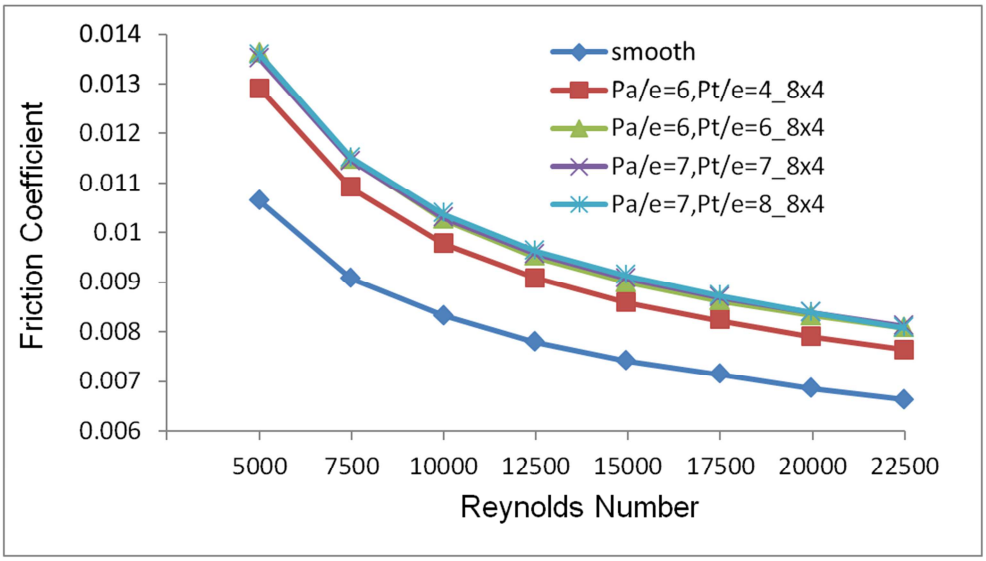

Figure 6. Comparison of friction co-efficient for different relative roughness pitch having fixed element size with smooth duct.

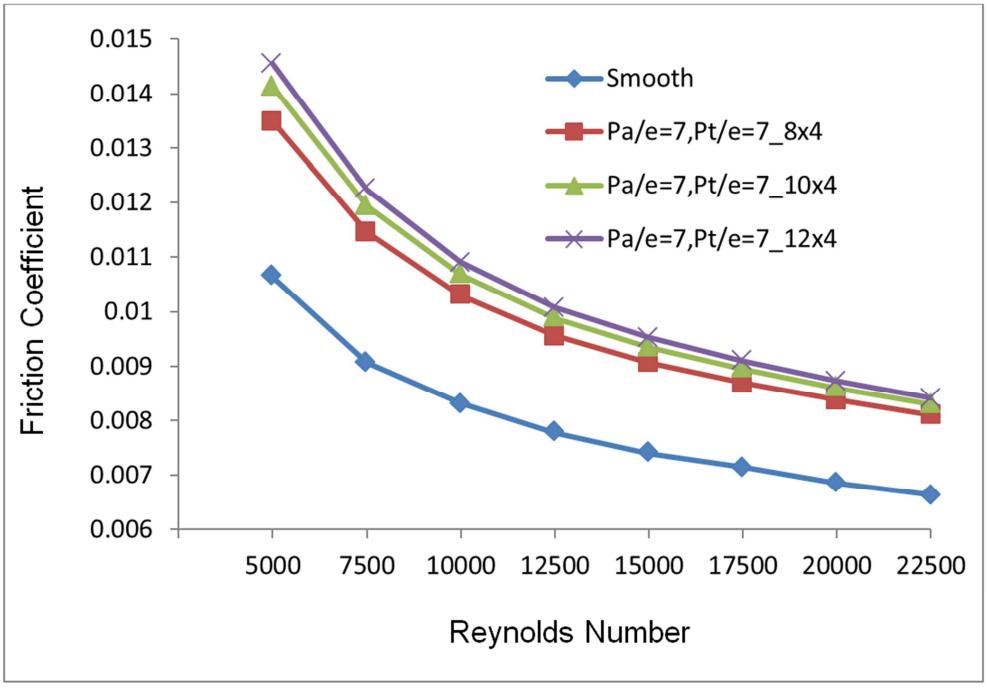

Figure 7. Comparison of friction co-efficient for different relative roughness pitch having fixed element size with smooth duct.

4.3. Overall Enhancement Ratio

The artificial roughness on the absorber plate of the SAH duct causes increase in the Nusselt number as well as the friction factor and pressure drop in the direction of flow. This increased friction in the flow requires more pumping power to drive the flow in the duct. Accordingly, in order to predict the overall performance of the duct, an overall enhancement ratio is defined as [21]

$$\text{Overall Enhancement Ratio} = = \frac{Nu_r / Nu_s}{\left(f_r / f_s\right)^{1/3}} \tag{8}$$

Figure 8 shows the variation of the overall enhancement ratio with Reynolds number for different roughness geometries. High value of this ratio represents an appreciable performance of the SAH duct. It is observed that for all Reynolds numbers the value of the overall enhancement ratio is greater than unity. Furthermore, for all different types of roughness geometry except Pa/e = 6 and Pt/e = 4 (with cross section 8×4), the value of overall enhancement ratio is the highest at Re = 5000. Thereafter it decreases sharply up to Re = 10000 and further there is a slight decrease. Again, it increases slightly for Re = 12500 to 22500. The SAH gives the best performance for the roughness geometry Pa/e = 7 and Pt/e = 7 (with cross section 12×4).

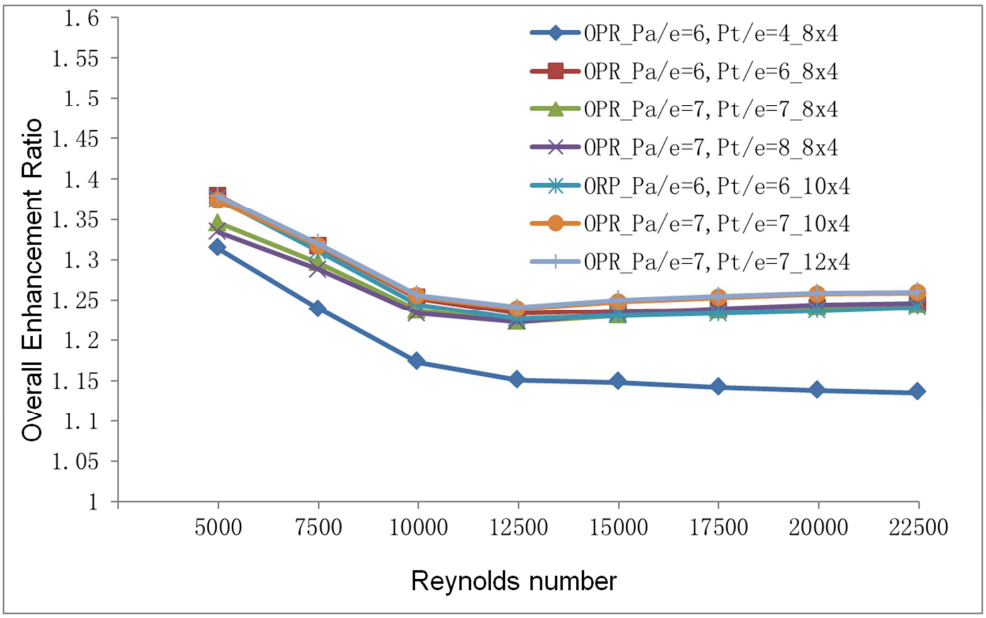

Figure 8. Variation of overall enhancement ratio with Reynolds number.

5. Conclusions

This paper presents a three-dimensional CFD investigation of the thermal hydraulic performance of the SAH having a rectangular duct with chamfered square roughness elements on the absorber plate. The major findings of the study are itemized below:

1. The thermal performance of the heater in presence of the chamfered square roughness elements is observed to be improved compared to the smooth duct based heater. The Nusselt number increases 1.36-1.54 times for the roughened heater compared to the smooth heater for the Reynolds number range used in the simulation.
2. The Nusselt number increases for the roughened absorber plate with increase in Reynolds number. The Nusselt number of the rough plate is in the range of 24.4 - 84.3 W/m^2K and for the smooth plate in range of 17.4-61.8 W/m^2K.
3. The friction co-efficient is found to increase for the roughened absorber plate in comparison to the smooth plate. It is in the range of 0.0076 - 0.0146 for the roughened plate, whereas 0.0066 - 0.0106 for the smooth plate. The increase in the friction co efficient is 1.33 times compared to 1.53 times increase in the Nusselt number.
4. Use of roughness geometry in SAH duct increases the Nusselt number and the friction factor in comparison to the smooth ducted heater. With the increase in the Reynolds number, the Nusselt number increases and the friction factor decreases for all combination of roughness geometry.
5. Roughness geometry having relative roughness pitch of 7 and 12 mm cube arm is found to have the best overall enhancement ratio.

References

[1] Hachemi A. Thermal performance enhancement of solar air heaters, by a fan-blown absorber plate with rectangular fins. Int. J. Energy Res. 1995; 19: 567-577.

[2] Chabane F, Moummi N, Benramache S. Experimental study of heat transfer and thermal performance with longitudinal fins of solar air heater. J. Adv. Res. 2014; 5: 183-192.

[3] Chabane F, Moummi N, Benramache S, Bensahal D, Belahssen O. Collector efficiency by single pass of solar air heaters with and without using fins. Eng. J. 2012; 17: 43-55.

[4] Ibrahim Z, Ibarahim Z, Yatim B, Ruslan H Md. Thermal efficiency of single-pass solar air collector. AIP Conference Proceedings 1571, 90 (2013); doi: 10.1063/1.4858635.

[5] Kasayapanand N, Kiatsiriroat T, Vorayos N. Enhanced heat transfer in a solar air heater with double-flow configuration by electrohydrodynamic technique. J. Enhanced Heat Transf. 2006; 13: 39-52.

[6] Roy A, Hoque E Md. Performance analysis of double pass solar air heater with packed bed porous media in Rajshahi. AIP Conference Proceedings 1851, 020010 (2017); https://doi.org/10.1063/1.4984639.

[7] Rajpoot SS, Koli DK. CFD analysis of solar air heater duct with rectangular rib surface. Int. J. Eng. Trends Tech. 2013; 4: 3006-3011.

[8] Dogra S. Effect of artificial roughness on thermal and thermohydraulic efficiency in rectangular duct of a double pass solar air heater by using transverse ribs on the absorber plate. Int. J. Mod. Eng. Res. 2013; 3: 2271-2274.

[9] Kumar TS, Thakur NS, Kumar A, Mittal V. Use of artificial roughness to enhance heat transfer in solar air heaters - a review. J. Energy Southern Africa 2010; 21: 35-51.

[10] Ansari OUH, Kalamkar VR. CFD analysis of solar air heater having absorber plate roughened with compound turbulators. Int. J. Eng. Dev. Res. 2017; 5: 40-58.

[11] Ranjan R, Paswan MK, Prasad N. CFD based analysis of a solar air heater having isosceles right triangle rib roughness on the absorber plate. Int. Energy J. 2017; 17: 57-74.

[12] Yadav AS, Thapak MK. Artificially roughened solar air heater: A comparative study. Int. J. Green Energy 2016; 13: 143-172.

[13] Vyas AA, Shringi D. CFD based thermal efficiency analysis of solar air heater with smooth plate and perforated plate. Imp. J. Interdisc. Res. 2017; 3: 415-422.

[14] Tapas V, Sao AK, Sharma P. Computational analysis of an artificial roughened surface of solar air heater. Int. J. Innovative Res. Sci. Eng. Tech. 2015; 4: 12205-12212.

[15] Prasad BN, Saini JS. Effect of artificial roughness on heat transfer and friction factor in a solar air heater. Solar Energy 1988; 41: 555-560.

[16] Karwa R, Bairwa RD, Jain BP, Karwa N. Experimental study of the effects of rib angle and discretization on heat transfer and friction in an asymmetrically heated rectangular duct. J. Enhanced Heat Transf. 2005; 12: 343–55.

[17] Karwa R, Srivastava V. Thermal performance of solar air heater having absorber plate with v-down discrete rib roughness for space-heating applications. J. Renew. Energy 2013; Article ID 151578: 1-13.

[18] Gawande VB, Dhoble AS, Zodpe, DB, Chamoli S. Analytical approach for evaluation of thermo hydraulic performance of roughened solar air heater. Case Studies Thermal Eng. 2016; 8: 19-31.

[19] ANSYS FLUENT 13.0 Theory Guide, ANSYS Inc., 2010.

[20] Thakur SK, Mittal V, Thakur NS, Kumar A. Heat transfer and friction factor correlations for rectangular solar air heater duct having 60° inclined continuous discrete rib arrangement. British J. Appl. Sci. Tech. 2011; 1: 67-93.

[21] Kumar M, Varun. A computational fluid dynamics investigation of solar air heater duct provided with inclined circular ribs as artificial roughness. Bonfring Int. J. Ind. Eng. Manag. Sci. 2014; 4: 115-120.